# Electroluminescence Studies on Self-Assembled Films of PPV and CdSe Nanoparticles

## Mingyuan Gao,* Bernd Richter, Stefan Kirstein, and Helmuth Möhwald

*Max-Planck-Institut für Kolloid- und Grenzflächenforschung, Rudower Chaussee 5, D-12489 Berlin, Germany*

*Received: January 5, 1998; In Final Form: March 16, 1998*

Electrooptical and structural studies on self-assembled films composed of CdSe nanoparticles, poly(*p*-phenylene vinylene) (PPV), and different nonconjugated polyelectrolytes are reported. It is demonstrated by optical spectroscopy and X-ray reflectivity measurements that CdSe nanoparticles and PPV can successfully be incorporated into homogeneous ultrathin films by the self-assembly method. The surface roughness obtained from the X-ray measurements is 2.7 and 1.3 nm respectively for CdSe/PAH (PAH, poly(allylamine) hydrochloride) and PSS/PPV (PSS, poly(styrenesulfonic acid)) multilayer films. This allows us to stack a (PSS/PPV)*n* film on top of a (CdSe/PAH)*n* film to build up well-defined two-layer composite film devices. Electroluminescence studies show that pure (PSS/PPV)*n* film devices exhibit green light emission but with a very short lifetime (several seconds) if operated in ambient air. During operation, the PPV emission shifts toward the blue, which indicates that the mean conjugation length of PPV is shortened due to oxidation. Oxidation of CdSe particles is also observed in (CdSe/PAH)*n* devices during operation. However, the stability of CdSe particles is enhanced if they are combined alternately with PPV, and a (CdSe/PPV)*n* device gives a broad, nearly white emission. The turn-on voltage of it is much smaller and better defined than that for a (CdSe/PAH)*20 device. This proves that PPV works like a charge-transportation layer rather than an emitting layer in the (CdSe/PPV)*n* film device. In an ITO//PEI(CdSe/PAH)*10/(PSS/PPV)*10//Al two-layer composite film device the lifetime of PPV electroluminescence can be prolonged for at least 1 order of magnitude only after the device is first operated under backward bias (positive pole on Al electrode). This suggests that the oxygen within the film is removed by this operation due to oxidation of the particles. Afterward, this two-layer composite film device presents emission from PPV and CdSe, respectively, when the sign of the external voltage is changed.

## Introduction

Because of the potential applications in large area display elements, the study of organic LEDs based on conjugated polymers has received more and more interest in the past years.[1−8] Organic conjugated polymers such as poly(*p*-phenylene vinylene) (PPV) and its derivatives have presented many advantages in electroluminescence applications because of their high fluorescence efficiency[9] and their good processability.[2,7,10] However, the long-term stability, color tunability, and quantum efficiencies of the organic LEDs still have to be improved. Therefore, not only the properties of organic conjugated materials must be enhanced, but it will also be necessary to combine it with other materials to improve the device characteristics.

Many materials, such as organic dyes,[11] porous silicon,[12] rare earth elements,[13] and conjugated polymers, etc., have been used as an emitting layer in electroluminescence devices. Recently, several groups have reported the use of II−VI semiconductor nanoparticles, such as CdSe, in combination with polymers in the manufacture of LEDs.[14−17] As a new type of optical material, semiconductor nanoparticles present very unique properties. Due to the quantum size effect, the absorption and fluorescence spectra of the Q-size semiconductor particles can easily be tuned. Additionally, the fluorescence efficiency and the stability of the nanoparticles can be greatly improved by modifying the particle surface.[18,19] These advantages make

nanoparticle material an ideal candidate for the use in electroluminescence applications. It has been demonstrated by Alivisatos et al. that electroluminescence from CdSe particles can be produced by combining the CdSe particles and PPV in a two-layer structure.[14] The emission wavelength of the CdSe could be tuned by using particles of different size.[14,15] The following outstanding features can therefore be expected when particles are used as an emitting layer in an organic/inorganic hybrid device: (1) since the emission wavelength can be controlled by the size of the particles, the chemical properties of the particles, and thus the process of device fabrication, remain unaltered for the fabrication of different colors; (2) various polymers may be used in combination with the particles to optimize the transport properties of electrons and holes, respectively; (3) the high fluorescence efficiency of semiconductor nanoparticle materials will contribute to improve the external quantum efficiency of such organic/inorganic hybrid devices.

A well-established self-assembly method (SA) was adopted to prepare all solid films for electroluminescence studies in this paper. The SA method is based on electrostatic attractions between oppositely charged species to build up ultrathin molecular films from aqueous solutions.[20−22] It has been demonstrated that by this method materials such as conductive polymers,[3,7,10] organic dyes,[21] and inorganic Q-particles[16,22−24] can be assembled into ultrathin films. This opens a route to combine different materials into a composite film and to build up two- or three-layer structured LEDs. Here, each layer itself consists of *n* self-assembled double layers, denoted as (N/P)*n*,

* Corresponding author. E-mail mingyuan@mpikg.fta-berlin.de, Fax 0049 30 6392 3102.

Self-Assembled Films of PPV and CdSe

*J. Phys. Chem. B, Vol. 102, No. 21, 1998* **4097**

where N represents the negatively and P the positively charged species. In this paper, structural and electroluminescence studies on (PSS/PPV)*$n$ (PSS, poly(styrenesulfonic acid), (CdSe/PPV)*$n$, (CdSe/PAH)*$n$ (PAH, poly(allylamine) hydrochloride), and (CdSe/PAH)*$n$/(PSS/PPV)*$n$ two-layer composite films are reported.

## Experimental Section

Cadmium perchlorate hydrate ($Cd(ClO_4)_2 \cdot XH_2O$, $X \sim 6$, Aldrich), thiolactic acid ($C_3H_6O_2S$, 95–97%, Sigma), aluminum selenide ($Al_2Se_3$, 99.9%, ABCR GmbH+Co.), phosphoric acid ($H_3PO_4$, Sigma, 85%), sodium hydroxide (NaOH, Aldrich, 99.99%), poly(ethylenimine) (PEI, Aldrich, 50%), and poly-(allylamine) hydrochloride (PAH, Aldrich, average $M_n$ 50 000–65 000) were used as received. Poly(styrenesulfonic acid) (PSS, Aldrich, MW ca. 70 000) was used after being dialyzed. The water used in all experiments is the Milli-Q water filtered with a 0.22 $\mu$m millistack filter at the outlet.

**1. Preparation of Negatively Charged CdSe Nanoparticles.** In principle, the CdSe particles with a negatively charged surface were prepared by treating $Cd^{2+}$ ions aqueous solution with $H_2Se$ gas in the presence of thiolactic acid. Shortly after the formation of the CdSe particles, a certain amount of NaOH solution and excess $Cd^{2+}$ were added to activate the CdSe particles. During this process, the thiolactic acid served as a stabilizing agent. The thiol group was binding at the surface of the particle and left the carboxylic group outside. Thus, the surface of the particles becomes negatively charged at high pH values. In our experiment, the pH value of the CdSe colloidal solution was controlled in a range of 9–10. The average diameter of the particles was measured as 4.9 nm with a standard deviation of 1.3 nm. Because of this relative large particle size distribution and the existence of surface defects, the CdSe sample presents a broad photoluminescence that looks nearly white in color. The details of the preparation and TEM characterization as well as the optical spectra of the CdSe nanoparticles are given in the Supporting Information.

**2. Preparation of Structurally Different Films by the Self-Assembly Method.** PEI was used as the first layer in all prepared films as reported elsewhere.[25] PAH and the precursor of PPV (pre-PPV) were used as positively charged species, and the negatively charged CdSe and PSS were adopted as oppositely charged species for the preparation of self-assembled films. Glass, ITO (indium tin oxide with 63 $\Omega$/□), and silicon wafer were selected as substrates for different experimental purposes. By repeatedly dipping the PEI-covered substrate into the PSS or CdSe and pre-PPV or PAH solution for definite times, films with defined structures were obtained.

In all experiments, the pre-PPV was converted into PPV by heating the films at 130 °C under $10^{-5}$ bar vacuum for 11 h after the film buildup was completed. The success of the transition can be seen from the difference of the absorption spectra of the film before and after elimination.

**3. Electroluminescence Measurements.** All electroluminescent devices were fabricated by integrating the SA films between the ITO and Al electrodes. A round-shaped Al electrode, 3 mm in diameter and 115 ± 15 nm in thickness, was prepared by vacuum evaporation. Gold and copper wires were used to contact the electrodes. $I-V$ measurements were performed with the help of a Keithley 617 electrometer. Electroluminescence was detected with a spectrometer consisting of a monochromator (SP275, Acton) and a thermoelectrically cooled CCD camera (S&I). Hence, the full spectrum was
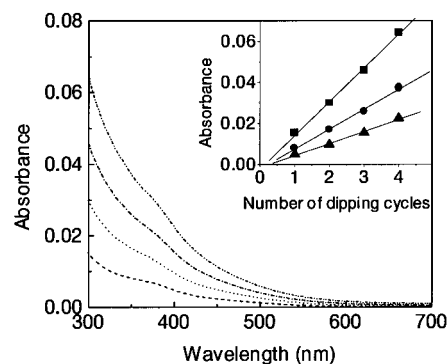


**Figure 1.** Absorption spectra of 1, 2, 3, and 4 double layer CdSe/PAH self-assembled films. Insert: absorbance at 300, 350, and 400 nm of (CdSe/PAH)*$n$ films against the number of dipping cycles.
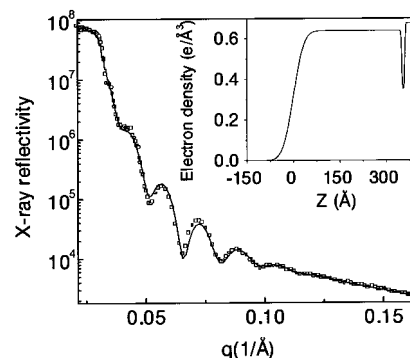


**Figure 2.** Experimental X-ray reflectivity data (small open squares) of a 12-double-layer CdSe/PAH film on silicon wafer. The solid line indicates a best fit according to the electron density profile shown in the insert. The Z-axis in the insert corresponds to the distance from air/film interface to film/substrate interface in the vertical direction of the film plane. A model that consists of three boxes, which correspond to the (PAH/CdSe)*12, PEI, and Si substrate respectively, is used. The thicknesses of the first two boxes are 34.9 and 1.0 nm with electron densities of 0.64 and 0.35 e/Å$^3$, respectively. The electron density of the substrate was taken as 0.68 e/Å$^3$. The roughness of each interface from air to substrate is 2.7, 0.2, and 0.2 nm, respectively.

recorded instantaneously. A fiber bundle was connected to the spectrometer, and the other end of the fiber was held directly in front of the LED device at the ITO side without any collimating optics.

**4. X-ray Reflectivity.** X-ray reflectivity measurements were performed with a commercial $\theta/2\theta$ instrument (STOE & CIE GmbH Darmstadt, $U = 40$ kV, $I = 50$ mA, $\lambda = 1.54$ Å (Cu K$\alpha$)). The divergence of the incoming beam was 0.1°, and the $2\theta$ resolution was 0.05°. The counting intervals are 3 s in $2\theta$ range of 0.3–0.8° and 10 s from 0.8° to 3°.

## Results

**1. Structure and Optical Spectra of Self-Assembled Films.** *a. (CdSe/PAH)*$n$ SA Films.* The absorption spectra of (CdSe/PAH)*$n$ films with different number of double layers are presented in Figure 1. The absorbance measured at 300, 350, and 400 nm is linearly increasing with the number of dipping cycles. This indicates that an equal amount of CdSe particles is adsorbed after each dipping cycle.

The (CdSe/PAH)*$n$ multilayer films deposited on silicon wafer were also characterized by X-ray reflectivity. In Figure 2 the measured reflectivity data are presented together with the best fit of a theoretical model. For the latter the electron density profile of the film along the direction vertical to the film plane is modeled by three independent boxes.[27] Each box is defined

by two parameters: the width, i.e., the layer thickness, and the height, i.e., the electron density of the layer. The first box represents the CdSe/PAH film, the second one describes the underlying PEI layer, and the third one corresponds to the silicon substrate. The boxes are blurred by a Gaussian function to account for the roughness of the surfaces and the interpenetrating of the PEI and CdSe/PAH layers. The reflectivity was calculated from the box model using the Fresnel equations.[28] A least-squares algorithm was used for the fitting procedure as described elsewhere.[29] The fits could be improved remarkably by introducing domains with reduced thickness in the film plane. These defects lead to a second reflected intensity that is incoherently superimposed to the reflectivity of the undisturbed areas. The mean surface coverage of the defects was estimated to be in the range of 0.5% for a 12-double-layer CdSe/PAH self-assembled film. Such domains can be assigned to an inhomogeneous distribution of the particles as was observed by transmission electron microscopy.

The electron density profile of the film that corresponds to the best fit is shown in the insert of Figure 2. A total film thickness of 34.9 nm and a surface roughness of 2.7 nm are obtained for the system of 12 double layers of CdSe/PAH. The thickness of the PEI layer is 1.0 nm. The electron densities are 0.64, 0.35, and 0.68 e/$Å^3$ for CdSe/PAH, PEI, and silicon substrate, respectively. The value for the substrate was taken from the literature.[27] Thus, the volume fraction of the CdSe particles in the CdSe/PAH film was estimated to be 23% using 1.46 and 0.4 e/$Å^3$ [30] for the electron density of CdSe and PAH, respectively.

The surface roughness extracted from a 6-double-layer CdSe/PAH film is 2.4 nm and nearly identical to that of a 12-double-layer CdSe/PAH film. This strongly indicates that there is no amplification of lateral defects within the layers during the film buildup. However, the average thickness of each double layer calculated from the reflectivity data is smaller than the average particle diameter. This means that the surface coverage of the particles is not high enough to form a complete layer.[23c,24] As a result, the particles of one layer fall into the gaps between the particles of the neighboring layers. In this way, no evident contrast of electron density exists between different layers, and thus no Bragg peaks appear in the reflectivity curve.

Pre-PPV was also used as a positively charged polyelectrolyte instead of PAH to build up the same structured films.[16] It turned out that there was no apparent difference regarding the film structures between the (CdSe/Pre-PPV)*$n$ and (CdSe/PAH)*$n$ multilayer films. For example, the difference in optical density of the CdSe particles in these two films, which had the same number of double layers, is less than 10%. In addition, under the same heating conditions for converting pre-PPV to PPV, no evident changes were found with the surface roughness of PPV/CdSe multilayer films. However, about 15% decrease of the film thickness was obtained. This is mainly due to the elimination reaction of pre-PPV. Similar decrease was also found with the PPV/PSS multilayer film after the heating treatment.

*b. (PSS/PPV)*$n$ *SA Films.* (PSS/PPV)*$n$ self-assembled films with different number of layers were prepared and converted under the conditions mentioned in the Experimental Section. The UV/vis absorption spectra of (PSS/PPV)*$n$ films are shown in Figure 3. An absorption peak with a maximum around 400 nm appeared after the heating treatment of the (PSS/pre-PPV)*$n$ SA films. This proves that the pre-PPV was successfully converted into the conjugated PPV under the selected elimination conditions. The structure of the (PSS/PPV)*$n$ films was
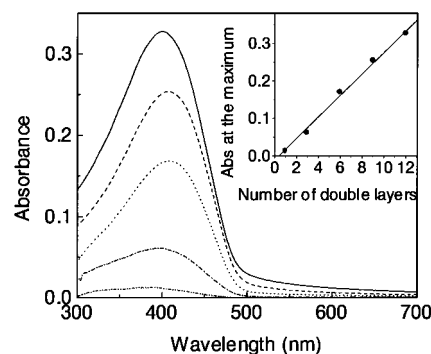


**Figure 3.** Absorption spectra of 1, 3, 6, 9, and 12 double layer PSS/PPV self-assembled films. Insert: absorbance of different films at the maximum position against the number of double layers.
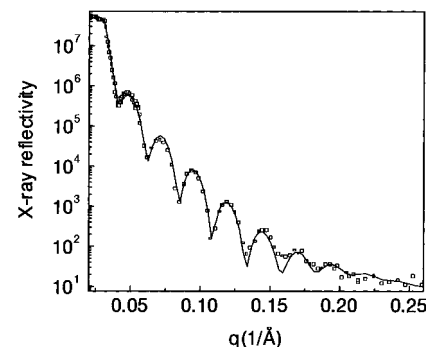


**Figure 4.** Experimental X-ray reflectivity data (small open squares) and best fit (solid line) of a 9-double-layer PSS/PPV self-assembled film. The fit is described by a simple box model assuming a thickness of 25.8 nm and a roughness at the film/air interface of 1.3 nm.

also characterized by the X-ray reflectivity method. The reflectivity curve of a 9-double-layer film together with a fit according to a simple box model is shown in Figure 4. The thickness of the film was 25.8 nm with a surface roughness of 1.3 nm.

The relatively small surface roughness of both (CdSe/PAH)*$n$ and (PSS/PPV)*$n$ multilayer films allowed us to position the (CdSe/PAH)*$n$ and (PSS/PPV)*$n$ multilayer films at a defined position in a composite film rather than to form a mixture of them. Hence, a (CdSe/PAH)*10/(PSS/PPV)*10 two-layer composite film was built up, which enables one to study the electroluminescence properties of the CdSe particles and PPV in one composite system.

**2. Electroluminescence of PPV and CdSe Particle Self-Assembled Film Devices.** As mentioned in the Experimental Section, ITO glass was used as the transparent electrode and also as the solid substrate for all LEDs' fabrication. After the SA films with a definite number of double layers were formed on the ITO glass that was initially covered with one layer of PEI, aluminum was evaporated directly on top of the film. All electroluminescence studies were performed in air at room temperature except for specially mentioned measurements.

*a. (PSS/PPV)*20 *SA Film Devices.* The typical $I-V$ characteristics of a 20-double-layer PSS/PPV LED are shown in Figure 5a, recorded under forward bias. In this paper, the forward bias is defined as the positive pole of the voltage source connected to the ITO electrode and the negative one to the Al electrode. As the voltage was raised, a small current peak at 6.5 V appeared, but only during the first voltage sweep. It was never observed during the subsequent measurements. Accompanying the appearance of the current peak, an El band at around 500 nm appeared and vanished with time, as shown in
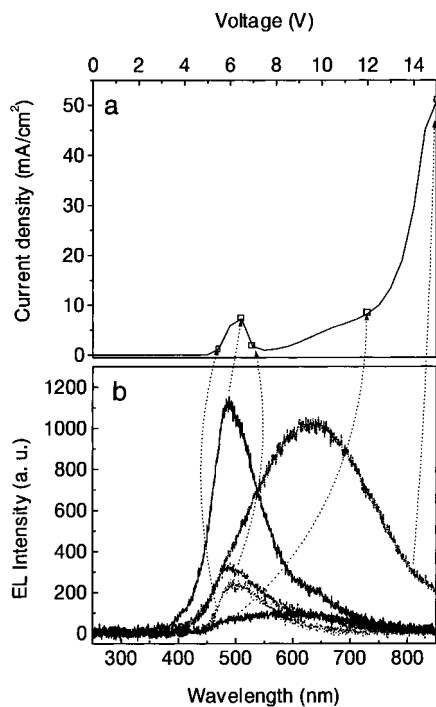
Self-Assembled Films of PPV and CdSe

*J. Phys. Chem. B, Vol. 102, No. 21, 1998* **4099**



**Figure 5.** (a) *I*−*V* characteristics of an ITO//PEI(PSS/PPV)*20//Al device recorded under forward bias. (b) Electroluminescence spectra of the ITO//PEI(PSS/PPV)*20//Al device recorded at different voltages at room temperature in air.



**Figure 6.** Electroluminescence spectra recorded from an ITO//PEI-(CdSe/PPV)*20//Al device under forward bias at room temperature in air. Insert: *I*−*V* and *I*−El intensity characteristics of the device.



**Figure 7.** (a) Fluorescence spectrum of a 12-double-layer CdSe/PPV film. (b) Fluorescence spectrum of a 12-double-layer CdSe/PAH film. (c) Fluorescence spectrum of the originally prepared CdSe particle solution. (d) One of the electroluminescence spectra of the ITO//PEI-(CdSe/PPV)*20//Al device recorded at room temperature in air.

Figure 5b. This emission band did not reappear on further increasing of voltage. Instead, a new emission band with a maximum of 650 nm arose under much higher operating voltage than 12 V. During subsequent measurements, only the second emission peak was observed with no evident changes. Thus, the green band at 500 nm, which resembles the fluorescence of PPV, had a lifetime of only several seconds for the in-air measurements. However, the second emission band was rather stable; it continuously emitted light for about 1 h. When observed under a fluorescence microscope, the second band emission was laterally homogeneous. Shortly before it disappeared, sparkles could be seen that show up in the El spectrum as sharp peaks. At the same time bubblelike defects on the Al electrode became observable to the naked eyes. Until now, the origin of the second band emission is unclear. However, in the electroluminescence spectra of thick films of pure PPV a similar red-shifted band is observed as a small peak that is absent in the fluorescence of PPV.[2b] This new band might be related to some changes of PPV during the El measurements, which become much significant in case of self-assembled film. Research on this subject is still on the way.

*b. (CdSe/PPV)*20 SA Film Devices.* The electroluminescence spectra recorded from a 20-double-layer CdSe/PPV film device under forward bias are shown in Figure 6. A broad emission band with the maximum around 657 nm appeared from 500 nm to the near-infrared region. The turn-on voltage under which a detectable spectrum can be captured is around 3.5 V.

Figure 7 presents the fluorescence spectra of the CdSe solution, a (CdSe/PAH)*12 film, a (CdSe/PPV)*12 film and one electroluminescence spectrum recorded from the (CdSe/PPV)*20 device. Clear shoulders at 500 and 535 nm, arising from PPV, appear in the fluorescence spectrum of the (CdSe/PPV)*12 film. Except for these differences all spectra are similar, which indicates that the electroluminescence of the (CdSe/PPV)*20 device comes from CdSe particles, rather than from PPV.
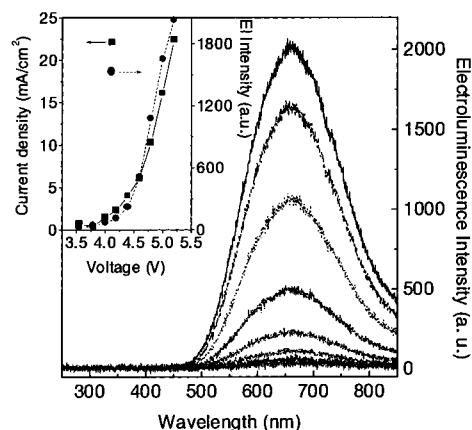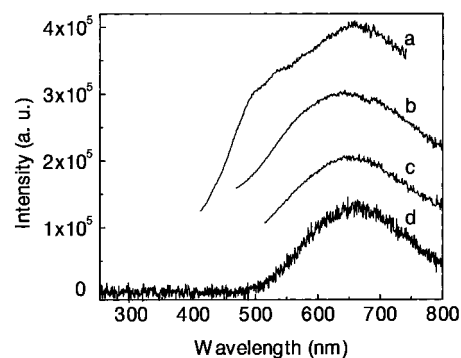
*c. (CdSe/PAH)*20 SA Film Device.* To understand the role of PPV in such an ITO//PEI(CdSe/PPV)*20//Al device, PAH was used instead of PPV to build up the same structured LED. A broad emission band with a maximum around 700 nm appeared above 10 V on increasing the voltage. At a certain threshold voltage (13.5 V) the *I*−*V* curve presents a jump to high current. This can be seen in Figure 8a. Here, the current is limited to 3.5 mA for higher voltages by the power supply. Accompanying this jump, a drastic increment of the El intensity appears as shown in Figure 8b. No changes was found for the emission maximum, but the onset of the emission at the blue side shifts toward 400 nm. A new emission band with a maximum around 550 nm becomes visible in the difference of the spectra recorded before and after the current jump. The mechanism of this current jump is not clear, but it may be the result of the appearance of some new current paths by burning the polymer between the electrode and particles. This model is confirmed by the fact that the jump in the *I*−*V* curve did not reappear when the voltage decreased from 15 to 0 V; see the dashed line in Figure 8a. This means that above some threshold voltage tunneling of charge carries from an electrode to the particles becomes very efficient. The dramatic increment of current density favors also the recombination of charge carriers at small particles, which contributes to the blue emission.

*d. (CdSe/PAH)*10/(PSS/PPV)*10 Two-Layer Composite SA Film Devices.* Devices with an ITO//PEI(CdSe/PAH)*10/(PSS/PPV)*10//Al structure were prepared by depositing 10 double layers of CdSe/PAH on top of ITO glass followed by 10 double layers of PSS/PPV and then evaporating Al on the top of the
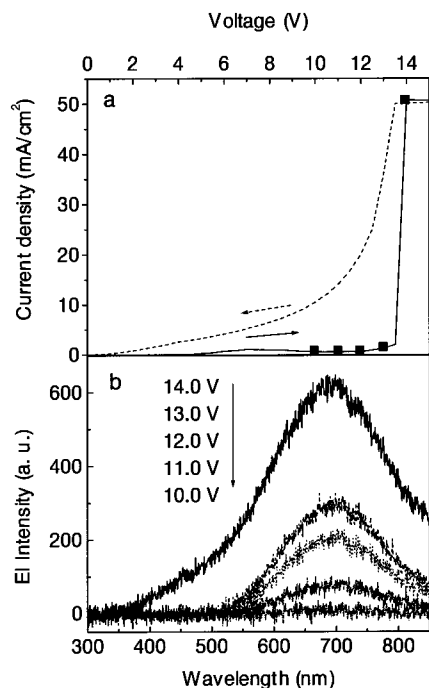
**Figure 8.** (a) $I-V$ curves of an ITO//PEI(CdSe/PAH)*20//Al device recorded in a cycle of 0 V → 15 V → 0 V (0 V → 15 V, solid line; 15 V → 0 V, dashed line). (b) Electroluminescence spectra of the ITO//PEI(CdSe/PAH)*20//Al device recorded under forward bias at room temperature in air. The spectra are recorded during the voltage increase process at the voltages marked as solid squares in frame a.

sample. Under forward bias, a fresh device showed very poor electroluminescence from PPV. After this measurement, visible damage can be observed on the aluminum electrode. However, when a new sample was first subject to backward bias, an emission from CdSe particles appeared. Then, a very strong and stable emission from PPV was observed when the LED was operated under forward bias again. This green emission turned out to be much more stable than that from the single-layer (PSS/PPV)*20 device. After these measurements, no visible damages on the electrode appeared. It was found out that in most cases the decline of the PPV emission from the (PSS/PPV)*20 and (CdSe/PAH)*10//(PSS/PPV)*10 devices was followed by the appearance of bubblelike defects on the aluminum electrode. Since no visible defect appears and strong PPV electroluminescence is emitted from the two-layer composite film device after the first operation under backward bias, it can be concluded that the appearance of the defects on Al is related to the degradation of PPV at the polymer/Al interface. However, after repeating several times the measurements under forward and backward bias alternately, defects appeared as colored rings near the edge, and small bubbles in the inner area of the electrode were observed with the sample that was first operated under backward bias; see Figure 9a. There are several possible reasons for the formation of these defects: (1) an edge effect[31] that will give enhanced electric fields and accelerate the degradation of PPV and CdSe particles at the edge area of the electrode; (2) the diffusion of oxygen from the ambient atmosphere will cause degradation of PPV as well as of CdSe particles preferentially near the device edge; (3) local heating[31] is suspected to be the possible reason for the formation of the small bubblelike defects in the inner area. However, the average size and the size distribution of these bubblelike defects are much smaller than that appearing on a composite film device after it was first operated under forward bias (Figure 9b). This indicates that proper polarity of the applied voltage during the
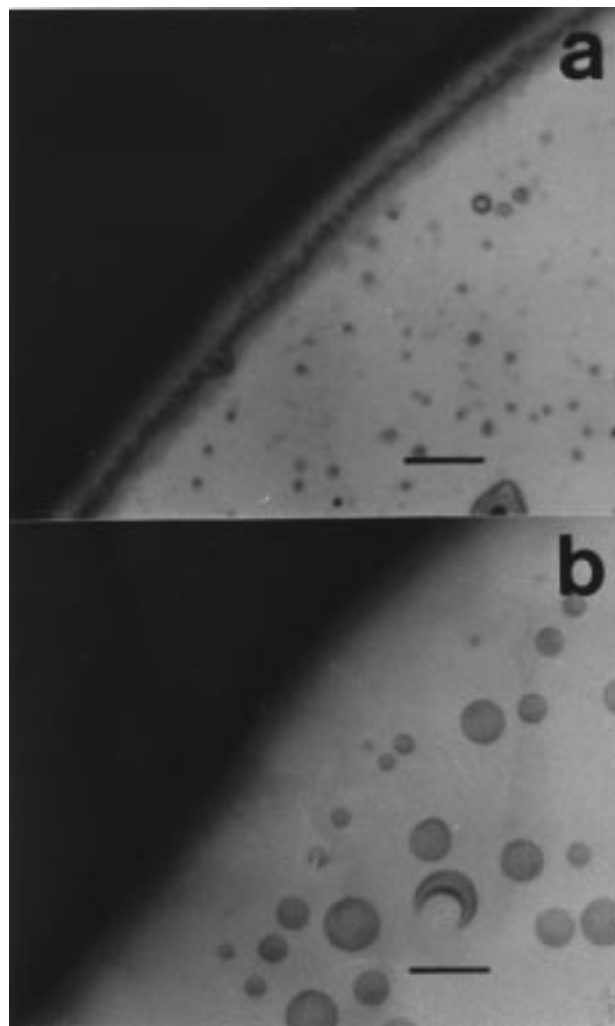


**Figure 9.** Micrograph of the Al electrodes on top of an ITO//PEI-(CdSe/PAH)*10/(PSS/PPV)*10//Al composite film device. The images were taken through the ITO electrode, and light gray areas correspond to the Al electrode. The scale bar is equal to 125 $\mu$m. (a) Electrode of a device that was first operated under backward bias and then five times alternately under different polarities. (b) Electrode of a device that was only one time operated under forward bias.

first operation on a freshly prepared composite film device is very important to prevent the PPV from degradation. Once a fresh two-layer composite film device was operated first under backward bias, one can switch several times the polarity of the external potential from forward bias that leads to PPV emission to backward bias that gives CdSe emission. However, the emission of PPV was broadened with time, and the emissions of CdSe shifts gradually to the red (see Figure 10). These spectral changes are also coupled with a slight decay in intensity.

## Discussion

**1. Stability of the (PSS/PPV)*20 Self-Assembled Film Device.** When operated in ambient conditions under forward bias, as mentioned in the Results section, a fresh (PSS/PPV)*20 SA film LED showed a very short lifetime of only several seconds. If the applied voltage was raised from 0 V with a small rate, such as 0.1 V/s, it was nearly impossible to capture a pronounced typical PPV emission spectrum. This implies that the degradation of the (PSS/PPV)*20 device is very fast. The typical El spectra of the (PSS/PPV)*20 device are shown in Figure 11a. The same spectra but normalized to the maximum are displayed in Figure 11b. All El spectra were recorded by
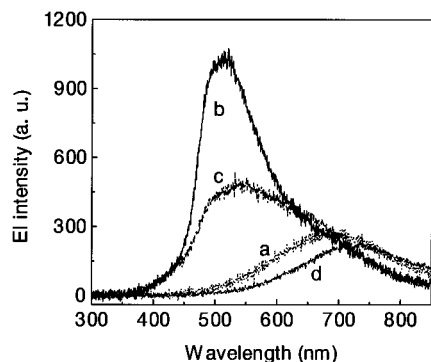
Self-Assembled Films of PPV and CdSe

*J. Phys. Chem. B, Vol. 102, No. 21, 1998* **4101**



**Figure 10.** Electroluminescence spectra recorded at room temperature in air of the composite film ITO//PEI(CdSe/PAH)*10/(PSS/PPV)*10//Al device. Spectrum a was measured from a fresh sample under backward bias, spectrum b during the subsequent operation under forward bias, and spectra c and d under forward and backward bias, respectively, after operations under alternating bias for five times.
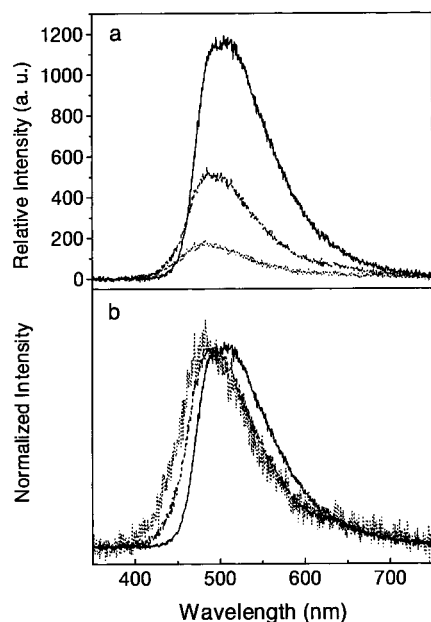


**Figure 11.** (a) Electroluminescence spectra of a fresh ITO//PEI(PSS/PPV)*20//Al device recorded under forward bias at room temperature in air. The externally applied voltage was 3.7 V, and the spectra were recorded in a time interval of 1 s. The recording sequence was from top to bottom. (b) Normalized spectra of that shown in frame a.

applying an external voltage of 3.7 V on a fresh sample. The emission significantly shifts toward the blue when the intensity decreases, as can be seen from Figure 11b. These results indicate that the conjugation length along the PPV chain was shortened by oxidation. Such an oxidation process has been demonstrated by Cumpston et al. when they studied the MEH-PPV devices by FTIR.[32a] As a result of the oxidation, carbonyl groups that can quench the fluorescence from PPV are generated.[33] Hence, in the presence of oxygen, the oxidation of PPV will shorten the lifetime of the PPV electroluminescence.

We did not try to increase the lifetime by preparing and measuring the LEDs of (PSS/PPV)*20 or (CdSe/PAH)*10/(PSS/PPV)*10 films in an oxygen-free environment, so there must be trace oxygen existing between the electrodes. It was also confirmed that when a fresh (PSS/PPV)*20 device was operated in helium after being stored in a vacuum for 12 h, the device presented a pronounced emission at around 500 nm for 2−3 min before the emission lost its original shape. This implies that one important reason for the short lifetime of the (PSS/
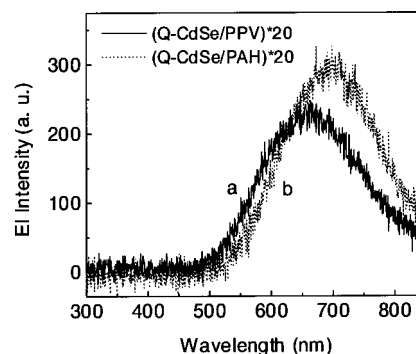


**Figure 12.** Electroluminescence spectra recorded under forward bias from an ITO//PEI(CdSe/PPV)*20//Al device (a) and an ITO//PEI(CdSe/PAH)*20//Al device (b).

PPV)*20 device is the oxidation of PPV under an external potential.

The short lifetime of our self-assembled PPV/PSS LEDs compared to that observed by other groups can be explained by the difference in the preparation conditions. One point is that we do not use any drying step after each deposition of a PSS/PPV double layer as was stated by Hong et al.[7] It was suggested there that the efficiency strongly depends on the drying procedure. On the other hand, it was demonstrated by Fou et al.[8] that the efficiency can be dramatically improved by the use of other polyelectrolytes instead of PSS. In this work, no effort was made to improve the stability of the single-layer (PPV/PSS)*n LEDs. This allowed us to demonstrate very clearly the improvement of the stability of the PPV emission by combining PPV with the CdSe particles.

**2. Electroluminescence of (CdSe/PPV)*20 and (CdSe/PAH)*20 Devices.** With respect to the electroluminescence properties of both of these two devices, two main differences can be found.

The first difference is that a much higher voltage is required to generate electroluminescence from (CdSe/PAH)*20 devices than from (CdSe/PPV)*20 devices. This indicates that in the former case charge carrier injection occurs mainly via PPV. Therefore, the injection of charge carriers at low voltage is very efficient. In the latter case a higher turn-on voltage is needed to inject charge carriers either into the nonconducting PAH or into the CdSe particles at a larger distance from the electrode. At the moment, these two alternatives cannot be distinguished. However, it can be concluded that PPV works as a transportation layer in the case of (CdSe/PPV)*20 devices. This is also supported by the experimental results that the electroluminescence comes from CdSe particles rather than PPV when they are alternately combined. This suggests that recombination of charge carriers only takes place at particles in contrast to the fluorescence emission, where luminescence from the PPV is also observed. The recombination of electrically injected charge carriers at the particles might be favored by Coulombic attraction between the carriers that are trapped at the particle surface and the free counterparts, since the particles have a large amount of defects at their surface for capturing the charge carriers and also a long lifetime of trapped states.

The second difference is that the maximum of the electroluminescence from the (CdSe/PAH)*20 shifts by about 50 nm to the red compared to the El from the (CdSe/PPV)*20 device, as shown in Figure 12. The red shift of the CdSe emission implies that there are some new deep trap sites formed on the surface of the particles during the measurements. A similar red shift was also observed with the electroluminescence spectra from the (CdSe/PPV)*20 device but only after the device was
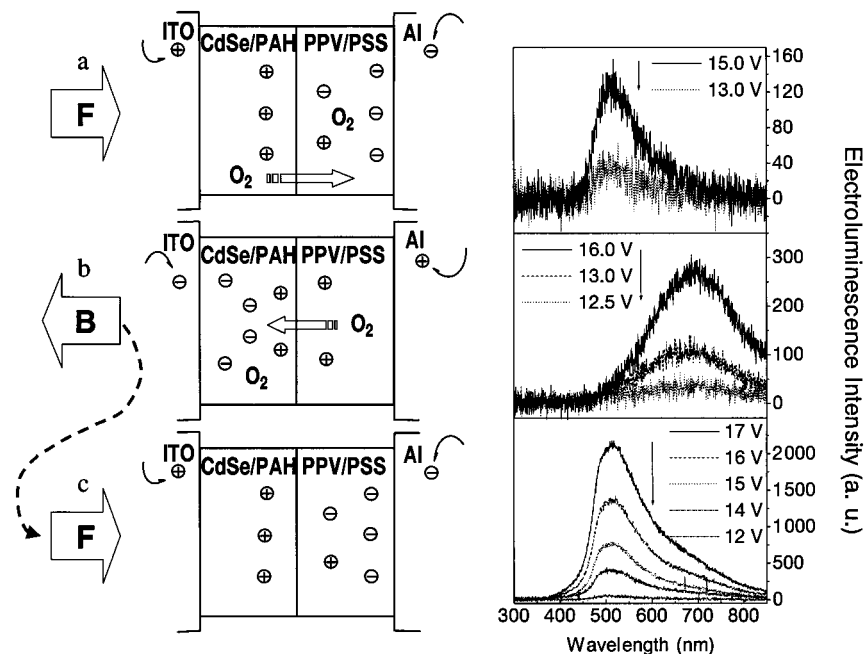
**Figure 13.** Schematic drawings of the structure of a ITO//PEI(CdSe/PAH)*10/(PSS/PPV)*10//Al two-layer composite film device (left). Electroluminescence spectra of the composite film devices (right) recorded at room temperature in air. The El spectra recorded from a fresh sample under forward bias are presented in the top frame. The El spectra recorded from a fresh sample under backward bias are presented in the middle frame, and the El spectra recorded under forward bias after the device was operated under backward bias are shown in the bottom frame. Note that the intensity of the electroluminescence spectra shown in the right-hand frames is comparable.

operated longer than 1 h. These results indicate that the CdSe−CdS core−shell particles are oxidized when they are excited under an external potential. It has been demonstrated by Weller et al.[18] that CdS nanoparticles can be oxidized in the presence of oxygen when the particles are excited by illumination; this is the so-called photooxidation process. However, PPV can prevent the CdSe from being oxidized when the CdSe particles and PPV are combined in an alternate way. As a result, the electroluminescence of a (CdSe/PPV)*20 device is nearly the same as the fluorescence of the CdSe particles in solution, in the (PAH/CdSe)*12, or in the (PPV/CdSe)*12 multilayer films.

**3. Electroluminescence of the (CdSe/PAH)*10/(PSS/PPV)*10 Two-Layer Composite Film Device.** As described in the Results section**,** the (CdSe/PAH)*10/(PSS/PPV)*10 two-layer composite film device produced a more stable electroluminescence than that from the (PSS/PPV)*20 device. But the prerequisite for this is to subject a freshly prepared two-layer composite film device first to backward bias. The proposed mechanism together with the electroluminescence spectra is outlined in Figure 13 and can be qualitatively understood as follows:

(a) When a freshly prepared sample was first operated under forward bias as shown in Figure 13a, the typical PPV emission appeared at around 490 nm above 13 V. The showing of this emission indicates that the recombination zone of charge carriers is located in the (PSS/PPV)*10 layer. PPV is a good hole conductor; hence, electrons injected into it do not travel far from the cathode. Therefore, with polarity of Figure 13a, electrons remain in the right part of the film. As a result, the recombination zone of the charge carriers is located in the (PSS/PPV)*10 layer.

As can also be seen in Figure 13a, the intensity of the PPV emission kept increasing until the voltage reached 15 V (the voltage-increasing rate is 0.5 V/s) and then decreased. The device presented a very short lifetime. The fast decline of the PPV emission is mainly due to the oxidation of PPV. It has been proven that the oxidation of PPV is one of the most

important reasons responsible for the failure of PPV devices.[32a] From the results of the IR studies on the photooxidation of BCHA-PPV, it is known that the appearance of singlet oxygen which was formed by energy transfer from the BCHA-PPV triplet state is responsible for the oxidation of BCHA-PPV.[32b] This suggests that once PPV is excited under an external potential, it will experience the same oxidation process as its photooxidation process in the presence of oxygen. When electroluminescence emits from a PPV device, the PPV singlet exciton state which is responsible for the electroluminescence and the PPV triplet exciton state will appear. Thus, reactive singlet oxygen that forms via energy transfer from PPV triplet exciton state will attack PPV and shorten its conjugation length.[32a]

It was also demonstrated that once a fresh sample was first operated under forward bias, it never gave the emission of PPV during subsequent measurements. After this operation, defects along the whole Al electrode were observed. The fast decline of the PPV emission and the appearance of the defects on the Al electrode proved that PPV was decomposed near the polymer/Al interface because of the oxidation reaction that occurred under current flow.

(b) However, when a fresh sample was first subjected to backward bias, as shown in Figure 13b, a broad emission that is identical to the emission of the (CdSe/PAH)*20 device appeared at 12.5 V. Even under higher operating voltage, there is no emission observed from PPV. This proved that the recombination zone is located in the (CdSe/PAH)*10 layer. PPV is good hole conductor. Holes injected from the Al electrode on the right side will quickly pass through the (PPV/PSS)*10 layer before the electrons injected from the ITO electrode on the left side arrive at the (PPV/PSS)*10 layer, so the recombination takes place in the (CdSe/PAH)*10 layer. Thus, the particles are excited and oxidized rather than PPV. In this way all oxygen present in the film will be consumed, but with less severe degradation of particles. After this backward bias operation, no visible defects on the Al electrode were observed.

(c) When such a sample that was preconditioned under backward bias was subject to forward bias, as shown in Figure 13c, it presented a very intensive and stable emission from PPV. Its lifetime was nearly the same as that of the (PSS/PPV)*20 device when the later was operated in helium after being stored in a vacuum for 12 h. This demonstrates that the oxygen presented in the film was consumed during the operation under backward bias. This allows one to create an oxygen-free environment within the film. For the further oxidation, the oxygen has to diffuse from the outside, a process that is very slow. This picture is supported by the degradation pattern of the Al electrode which starts to decompose mainly from the border and not throughout the whole area, as shown in Figure 9a.

## Summary and Conclusions

Different kinds of self-assembled film LEDs have been constructed using PPV, CdSe nanoparticles, and other poly-electrolytes. Since the (PSS/PPV)*n and (CdSe/PAH)*n films show a relatively small surface roughness, they can be placed on top of each other to form a (CdSe/PAH)*n/(PSS/PPV)*n two-layer composite film. In ambient conditions, the single-layer (PSS/PPV)*n SA film device produced a green light emission from PPV. Because of oxidation of PPV under the external potential, the device presented short lifetimes. However, the lifetime of the PPV electroluminescence was enhanced when the (PSS/PPV)*n film was built on top of the (CdSe/PAH)*n SA film, but only after the composite film device was first operated under backward bias. This strongly proved that, under backward bias, trace oxygen was consumed by the CdSe particles. However, this did not significantly change the transportation and emission properties of the particles. During subsequent operation under forward bias the emission of PPV from the composite film device became as stable as that from a single-layer (PSS/PPV)*n device when the latter was operated in helium after being stored in a vacuum.

Oxidation of CdSe particles was also observed when a (CdSe/PAH)*n device was operated. On the contrary, when the CdSe particles were alternately combined with PPV, the oxidation of CdSe particles also became not evident. In conclusion, the combination of CdSe nanoparticles and PPV is beneficial for both of them regarding the stability of the electroluminescence. We want to note that the stabilization effect reported here may be extended to other systems and be useful from a very general point of view.

**Supporting Information Available:** Preparation, characterization, and optical spectroscopic results of CdSe nanoparticles; detail preparation conditions for structurally different multilayer self-assembled films (2 pages). Ordering information is given on any current masthead page.

## References and Notes

(1) (a) Burroughes, J. H.; Bradley, D. D. C.; Brown, A. R.; Marks, R. N.; Mackay, K.; Friend, R. H.; Burns, P. L.; Holmes, A. B. *Nature* **1990**, *347*, 539. (b) Brown, A. R.; Greenham, N. C.; Burroughes, J. H.; Bradley, D. D. C.; Friend, R. H.; Burn, P. L.; Kraft A.; Holmes, A. B. *Chem. Phys. Lett.* **1992**. *200*, 46.

(2) (a) Herold, M.; Gmeiner, J.; Schwoerer, M. *Acta Polym.* **1994**, *45*, 392. (b) Herold, M.; Gmeiner, J.; Schwoerer, M. *Acta Polym.* **1996**, *47*, 436.

(3) (a) Tian, J.; Wu, C. C.; Thompson, M. E.; Sturm J. C.; Register, R. A. *Chem. Mater.* **1995**, *7*, 2190. (b) Tian, J.; Wu, C. C.; Thompson, M. E.; Sturm, J. C.; Register, R. A.; Marsella, M. J.; Swager, T. M. *Adv. Mater.* **1995**, *7*, 395.

(4) (a) Zhang, C.; Braun, D.; Heeger, A. J. *J. Appl. Phys.* **1993**, *73*, 5177. (b) Braun, D.; Heeger, A. J. *Appl. Phys. Lett.* **1991**, *58*, 1982.

(5) Garten, F.; Hiberer, A.; Cacialli, F.; Esselink, E.; Dam, Y. *Adv. Mater.* **1997**, *9*, 127.

(6) Bolognesi, A.; Bajo, G.; Paloheimo, J.; Östergard T.; Stubb, H. *Adv. Mater.* **1997**, *9*, 121.

(7) (a) Hong, H.; Davidov, D.; Avny, Y.; Chayet, H.; Faraggi, E. Z.; Neumann, R. *Adv. Mater.* **1995**, *7*, 846. (b) Faraggi, E. Z.; Chayet, H.; Davidov, D.; Avny, Y.; Newmann, R. *Synth. Met.* **1997**, *85*, 1247. (c) Hong, H.; Davidov, D.; Tarabia, M.; Chayet, H.; Benjiamin, I.; Faraggi, E. Z.; Avny, Y.; Neumann, R. *Synth. Met.* **1997**, *85*, 1265. (d) Noach, S.; Faraggi, E. Z.; Cohen, G.; Avny, Y.; Neumann, R.; Davidov, D.; Lewis, A. *Appl. Phys. Lett.* **1996**, *69*, 3650.

(8) Fou, A. C.; Onitsuka, O.; Ferreira, M.; Rubner, M. F. *J. Appl. Phys.* **1996**, *79*, 7501.

(9) (a) Greenham, N. C.; Samuel, I. D. W.; Hayes, G. R.; Phillips, R. T.; Kessener, Y. A. R. R.; Moratti, S. C.; Holmes, A. B.; Friend, R. H. *Chem. Phys. Lett.* **1995**, *241*, 89. (b) Peng, X. G.; Schlamp, M. C.; Kadavanich, A. V.; Alivisatos, A. P. *J. Am. Chem. Soc.* **1997**, *119*, 7019.

(10) (a) Cheung, J. H.; Stockton, W. B.; Rubner, M. F. *Macromolecules* **1997**, *30*, 2712. (b) Stockton, W. B.; Rubner, M. F. *Macromolecules* **1997**, *30*, 2717. (c) Fou, A. C.; Rubner, M. F. *Macromolecules* **1995**, *28*, 7115. (d) Ferreira, M.; Rubner, M. F. *Macromolecules* **1995**, *28*, 7107.

(11) Salbeck, J. *Ber. Bunsen-Ges. Phys. Chem.* **1996**, *100*, 1667.

(12) (a) Koshida N.; Koyama, H. *Appl. Phys. Lett.* **1992**, *60*, 347. (b) Li, K. L.; Diaz, D. C.; He, Y.; Campbell, J. C.; Tsai, C. *Appl. Phys. Lett.* **1994**, *64*, 2394.

(13) (a) Kido, J.; Hayase, H.; Hongawa, K.; Nagai, K.; Okuyama, K. *Appl. Phys. Lett.* **1994**, *65*, 2124. (b) Sohn, S. H.; Hamakawa, Y. *Appl. Phys. Lett.* **1993**, *62*, 2242.

(14) Colvin, V. L.; Schlamp, M. C.; Alivisatos, A. P. *Nature* **1994**, *370*, 354.

(15) Dabbousi, B. O.; Bawendi, M. G.; Onitsuka, O.; Rubner, M. F. *Appl. Phys. Lett.* **1995**, *66*, 1316.

(16) Gao, M. Y.; Richter, B.; Kirstein, S. *Adv. Mater.* **1997**, *9*, 802.

(17) Yang, Y.; Xue, S.; Liu, S.; Huang, J.; Shen, J. C. *Appl. Phys. Lett.* **1996**, *69*, 377.

(18) Spanhel, L.; Haase, M.; Weller, H.; Henglein, A. *J. Am. Chem. Soc.* **1987**, *109*, 5649.

(19) Hines, M. A.; Guyot-Sionnest, P. *J. Phys. Chem.* **1996**, *100*, 468.

(20) (a) Decher, G.; Hong, J. D. *Ber. Bunsen-Ges. Phys. Chem.* **1991**, *95*, 1430. (b) Decher, G.; Hong, J. D. *Makromol. Chem., Macromol. Symp.* **1991**, *46*, 321. (c) Decher, G.; Lvov, Y.; Schmitt, J. *Thin Solid Films* **1994**, *244*, 772.

(21) (a) Zhang, X.; Kong, X. X.; Sun, Y. P.; Shen, J. C. *J. Chem. Soc., Chem. Commun.* **1994**, 1055. (b) Sun, C. C.; Sun, Y. P.; Zhang, X.; Xu, H. D.; Shen, J. C. *Anal. Chim. Acta* **1995**, *312,* 207. (c) Copper, T. M.; Campbell, A. L.; Grane, R. L. *Langmuir* **1995**, *11*, 2713.

(22) (a) Fendler, J. H.; Meldrum, F. C. *Adv. Mater.* **1995**, *7*, 607. (b) Kotov, N. A.; Dekany, I.; Fendler, J. H. *J. Phys. Chem.* **1995**, *99*, 13065.

(23) (a) Gao, M. Y.; Zhang, X.; Yang, B.; Shen, J. C. *J. Chem. Soc., Chem. Commun.* **1994**, 2229. (b) Gao, M. Y.; Gao, M. L.; Zhang, X.; Yang, Y.; Yang, B.; Shen, J. C. *J. Chem. Soc., Chem. Commun.* **1994**, 2777. (c) Gao, M. Y.; Zhang, X.; Yang, B.; Li, F.; Shen, J. C. *Thin Solid Films* **1996**, *284−285*, 242.

(24) Schmitt, J.; Decher, G. *Adv. Mater.* **1997**, *9*, 61.

(25) Lehr, B.; Seufert, M.; Wenz, M.; Decher, G. *Surpramol. Sci.* **1996**, *2*, 199.

(26) Murray, C. B.; Norris, D. J.; Bawendi, M. G. *J. Am. Chem. Soc.* **1993**, *115*, 8706.

(27) Russell, T. P. *Mater. Sci. Rep.* **1990**, *5*, 171.

(28) Parrat, L. G. *Phys. Rev.* **1954**, *95*, 359.

(29) Asmussen, A.; Riegler, H. *J. Chem. Phys.* **1996**, *104*, 8159.

(30) Schmitt, J.; Grunewald, T.; Decher, G.; Pershan, P. S.; Kjaer, K.; Losche, M. *Macromolecules* **1993**, *26*, 7058.

(31) Burrows, P. E.; Bulovic, V.; Forrest, S. R.; Sapochak, L. S.; McCarty, D. M.; Thompson, M. E. *Appl. Phys. Lett.* **1994**, *65*, 2922.

(32) (a) Cumpston, B. H.; Parker, I. D.; Jensen, K. F. *J. Appl. Phys.* **1997**, *81*, 15. (b) Cumpston, B. H.; Jensen, K. F. *Synth. Met.* **1995**, *73*, 195.

(33) (a) Scot, J. C.; Kaufman, J. H.; Brock, P. J.; DiPietro, R.; Salem, J.; Goitia, J. A. *J. Appl. Phys.* **1996**, *79*, 2745. (b) Papadimitrakopoulos, F.; Konstadinidis, K.; Miler, T. M.; Opila, R.; Chandross, E. A.; Galvin, M. E. *Chem. Mater.* **1994**, *6*, 1563.

(34) Majetich, S.; Newbury, J.; Newbury, D. *Mater. Res. Soc. Symp. Proc.* **1994**, *332*, 321.